# Explaining the Sensitivity of Polymer Segmental Relaxation to Additive Size Based on the Localization Model

Thomas Q. McKenzie-Smith,[1] Jack F. Douglas,[2] and Francis W. Starr[1]
[1]Department of Physics, Wesleyan University, Middletown, Connecticut 06459-0155, USA
[2]Materials Science and Engineering Division, National Institute of Standards and Technology, Gaithersburg, Maryland 20899, USA

(Received 24 July 2021; revised 20 October 2021; accepted 14 December 2021; published 30 December 2021)

We use molecular simulations to examine how the dynamics of a coarse-grained polymer melt are altered by additives of variable size and interaction strength with the polymer matrix. The effect of diluent size $\sigma$ on polymer dynamics changes significantly when its size is comparable to the polymer segment size. For each $\sigma$, we show that the localization model (LM) quantitatively describes the dependence of the segmental relaxation time $\tau$ on temperature $T$ in terms of dynamic free volume, quantified by the Debye-Waller factor $\langle u^2 \rangle$. Within this model, we show that the additive size alone controls the functional form of the $T$ dependence. The LM parameters reach asymptotic values when the diluent size exceeds the monomer size, converging to a limit applicable to macroscopic interfaces.

DOI: 10.1103/PhysRevLett.127.277802

Adding particles of various sizes and interaction strengths has long been utilized to alter the dynamical and mechanical properties of polymer materials. This tunability is used in a myriad of applications, from building flexible integrated circuits to preserving biomaterials [1–7]. These additives can vary greatly in size, ranging from the molecular scale ($\lesssim$1 nm) to the scale of nanoparticles ($\gtrsim$2 nm). The case of nanoparticle (NP) additives has been extensively studied, and it is known that attractive interactions between the polymer and NP diminish the polymer mobility in an interfacial zone, which results in an overall slowing of composite dynamics [8,9]. Similar changes to polymer dynamics occur in polymer thin films, and these films can be roughly considered as the limit of NP with infinite radius [8,10]. This slowing of segmental dynamics carries over to smaller, attractive, molecular-scale additives [11]. On the other hand, small additives with a weaker attraction to the polymer matrix can enhance polymer mobility and reduce viscosity, commonly referred to as plasticization [12–15]. For these molecular-scale additives ("diluents"), the polymer mobility has been shown to depend on additive size. For additives smaller than the size of polymer segments, Varnik and co-workers recently used molecular simulations to show that dynamics can vary nonmonotonically with additive size [13,16]. Experimentally, there is evidence that additives with a size comparable to that of polymer segments can give rise to large changes in dynamics [11] and gas permeability [17–19]. Motivated by these considerations, we investigate the changes in the polymer dynamics for additive sizes ranging from molecular-scale (smaller than polymer segments) to NP-scale (larger than segments) and show that changes can be directly explained in terms of a dynamic free volume through the localization model (LM) [12,20,21].

To understand the effects of additive size, we examine changes in composite dynamics using additive sizes from about half a monomer diameter ($\sigma = 0.6$) to twice the monomer diameter ($\sigma = 2.0$). At small sizes, interfacial effects are negligible, yet we still find substantial, size-dependent changes to dynamics compared to a pure (no additive) system. This large effect of small additives on dynamics is consistent with other simulation studies [12–16] and experiments [11]. Experimentally measured changes of gas permeability due to additives have been shown to parallel changes in the positron volume [17–19], which in turn correlate with the amplitude of molecular vibrations quantified by the Debye-Waller factor $\langle u^2 \rangle$ [22]. Thus, to better understand the additive size-dependent alteration of the polymer dynamics, we turn to the LM, which posits a link between the segmental, $\alpha$-timescale relaxation $\tau$ and Debye-Waller factor $\langle u^2 \rangle$ [12,20,21]. Although $\tau$ and $\langle u^2 \rangle$ show qualitatively different $\sigma$ dependence at low and high $T$, we find that the LM is remarkably successful at relating the $T$ dependence of $\tau$ to $\langle u^2 \rangle$ for any given additive size $\sigma$. Furthermore, for $\sigma$ larger than the monomer diameter, we find the parameters of the LM are independent of additive size, suggesting that the transition from molecular to NP-scale additives is associated with a transition from a $\sigma$-dependent to a $\sigma$-independent LM description, and that this transition occurs for a surprisingly small additive size.

Our findings are based on molecular simulations of a bulk polymer system of 600 chains of length 10 (below the entanglement length) with spherical additives, carried out using the LAMMPS molecular dynamics simulation package [23]. Additives and polymer beads interact via the Lennard-Jones

 

(LJ) potential. Interactions among monomers of the chains define reference values for the LJ potential, $\epsilon_{mm} = \sigma_{mm} = 1$ ($mm$ is monomer-monomer, $ma$ is monomer-additive, and $aa$ is additive-additive); for additive-additive interactions, $\sigma_{aa}$ ranges from 0.6 to 2 $\sigma_{mm}$; for monomer-additive interactions, $\sigma_{ma}$ is the average of $\sigma_{aa}$ and $\sigma_{mm}$, following the standard Lorentz rule. We truncate and shift the LJ potential at 2.5 times the corresponding LJ diameter of the pair. The primary results examine additives with a fixed interaction strength for all $\sigma_{aa}$ to separate the effect of additive size from the better known effects of attraction strength; specifically, we choose $\epsilon_{aa} = 1.0$ and $\epsilon_{ma} = 1.5$ to ensure that additives do not phase separate from the polymer matrix. Motivated by the experimentally known dependence of the LJ parameters of hydrocarbons [24–27], we perform a more limited set of simulations in which the attraction strength varies linearly with the additive size; specifically, we define $\epsilon_{aa} = \epsilon_0(2\sigma_{aa} - \sigma_0)$, with the polymer-additive interaction strength $\epsilon_{ma}$ following the Berthelot geometric mean mixing rule. We choose $\epsilon_0 = 2.25$ and $\sigma_0 = 1.0$ so that additive size $\sigma_{aa} = 1$ has the same $\epsilon_{ma}$ as our primary results with fixed $\epsilon_{ma}$. These additional simulations allow us to mimic experimentally available additives, while also testing the sensitivity of our findings to the interaction strength. Regardless of size, all particles have mass 1.0. To simplify notation, all units are henceforth reported relative to the polymer values $\sigma_{mm} = \epsilon_{mm} = 1$, and we relabel the additive diameter $\sigma_{aa}$ to $\sigma$, since it is the only size that varies. Bonded polymer beads also interact via a harmonic potential $V = \frac{1}{2}k_{\text{chain}}(r - r_0)^2$, where $k_{\text{chain}} = 1111\epsilon_{mm}$ and $r_0 = 0.9\sigma_{mm}$ [28,29]. The largest additive size bridges the gap between small, molecular diluents and the variable size nanoparticles studied in our previous Letter [30].

To isolate the effects of additive diameter $\sigma$, we keep the volume occupied by additive particles relative to that of all particles fixed. Specifically, we restrict ourselves to a representative additive volume fraction $v = N_a\sigma^3/(N_m + N_a\sigma^3) = 0.1$, typical for many applications. Thus, we use more additives for small $\sigma$ to maintain constant $v$. At $v = 10\%$, the number of additives ranges from 83 for the largest $\sigma = 2.0$ to 3086 additives for the smallest $\sigma = 0.6$. For each $\sigma$, we simulate the system from temperature $T = 0.40$ to 1.2 along an isobaric path with pressure $P = 0$. The lowest temperature $T$ simulated is limited by time needed to equilibrate systems using typical GPU computing resources currently available.

We characterize polymer and additive $\alpha$-relaxation dynamics by examining the self part of the intermediate scattering function

$$F_{\text{self}}(q,t) = \frac{1}{N}\left\langle \sum_{j=1}^{N} e^{-i\mathbf{q}\cdot[\mathbf{r}_j(t)-\mathbf{r}_j(0)]} \right\rangle, \tag{1}$$

where $\mathbf{q}$ is the scattering vector. Following common practice, we evaluate $F_{\text{self}}(q,t)$ at $q = q_0$, the primary peak of the monomer structure factor (see Supplemental Material [31]). Figure 1 shows the $\sigma$ dependence of $F_{\text{self}}(q_0,t)$ at the relatively low temperature $T = 0.45$ for both the polymer and additives for the case of additives with a fixed interaction strength (see Supplemental Material [31] for the case of variable interaction strength). At vibrational timescales ($t \lesssim 1$), Fig. 1(a) shows that the relaxation rate of monomers increases with increasing $\sigma$. In contrast, the additives [Fig. 1(b)] show the opposite $\sigma$ dependence. Approaching the $\alpha$-relaxation timescale, $F_{\text{self}}(q_0,t)$ for different $\sigma$ cross each other, both for polymer segmental relaxation and additive relaxation. As a consequence, there is a complex $\sigma$ dependence of $\alpha$ relaxation.

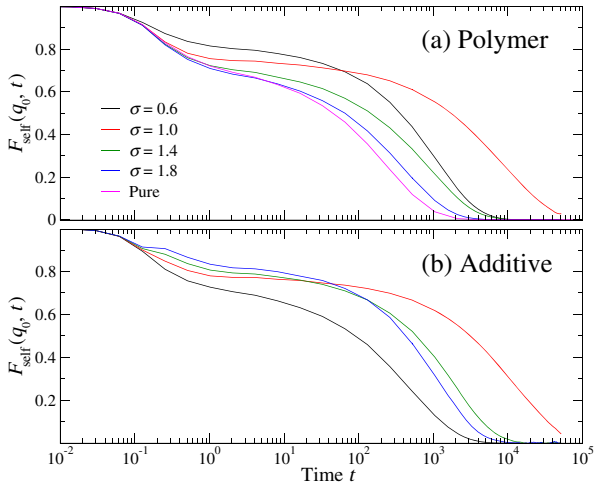


FIG. 1. The relaxation of $F_{\text{self}}(q_0,t)$ for (a) monomers and (b) additives for representative $\sigma$ values, including a comparison to the pure system. All data are taken at $T = 0.45$. These data are for fixed $\epsilon_{ma}$; similar data for variable $\epsilon_{ma}$ are provided in the Supplemental Material [31].

We can capture the complex dependence of the relaxation more clearly via the $\alpha$-relaxation time $\tau$. Following a common convention, we define $F_{\text{self}}(q,\tau) = 0.2$, noting that our qualitative findings are insensitive to the definition of $\tau$; $\tau_m$ and $\tau_a$ define the relaxation time for monomers and additives, respectively. For both the case of fixed and variable interaction strength $\epsilon_{ma}$, Figs. 2(a) and 2(b) show that $\tau_m$ and $\tau_a$ both increase significantly with increasing $\sigma$ up to $\sigma \approx 1.0$, the monomer scale. For fixed $\epsilon_{ma}$, $\tau$ reaches a maximum and decreases for $\sigma > 1.0$; for variable $\epsilon_{ma}$, $\tau$ reaches an approximate plateau for $\sigma > 1.0$. Note that, in the case of variable $\epsilon_{aa}$, there is an implied minimum in $\tau$ for $\sigma < 0.6$, since $\tau$ at $\sigma = 0.6$ is smaller than the pure melt, and we expect to smoothly recover the behavior of the pure melt in the limit of vanishing additive size. Curiously, in all cases, the polymer segments and additives have the same relaxation time at $\sigma \approx 0.85$, a point to which we shall return. It is not readily apparent why both $\tau_m$ and $\tau_a$ should increase dramatically only until a size comparable to the monomer

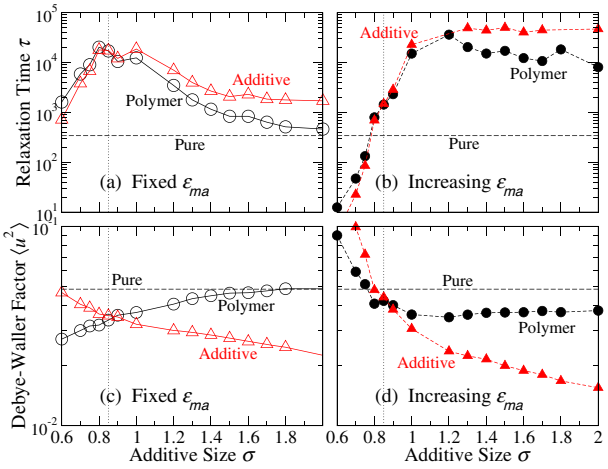


FIG. 2. (a),(b) Segmental relaxation time $\tau$ for polymer (black circles) and additives (red triangles) as a function of additive size at $T = 0.45$ for (a) fixed monomer-additive interaction strength $\epsilon_{ma}$ and (b) variable $\epsilon_{ma}$. The horizontal dashed line is the reference value for the pure polymer system. (c),(d) Debye-Waller factor $\langle u^2 \rangle$ as a function of additive size at $T = 0.45$ for (c) fixed $\epsilon_{ma}$ and (d) variable $\epsilon_{ma}$.

diameter. However, this qualitative change in $\tau$ does seem quite general. In fact, Varnik and co-workers [13,16] previously observed a local maximum in the segmental relaxation time at nearly the same additive size in simulations using a similar model. Combined with our results, this suggests that the qualitative change in segmental relaxation time at $\sigma \approx 1$ (the segment size) does not depend significantly on additive interactions. Because of this, we conclude that this characteristic size scale arises from considerations related to packing (controlled by additive size) rather than the specific interactions. This is also consistent with the experiments of Cheng *et al.* [11], who observed a large slowing of nanocomposite segmental dynamics using attractive additives with a diameter similar to the segmental size and reported a diminished effect for larger nanoparticles.

Naively, one might expect this packing effect on relaxation to be controlled by changes in the overall packing fraction. However, choosing a fixed $v = 10\%$, the packing fraction does not reflect the $\sigma$-dependent changes of $\tau$ (see Supplemental Material [31]). Thus, simplistic free volume ideas based on average density are insufficient to account for these dynamical changes. To explain the variations in local packing that lead to the observed trends in the relaxation times, we use a local dynamic measure of accessible volume, which is linked to the $\alpha$ relaxation through the localization model. This accessible volume is quantified by $\langle u^2 \rangle^{3/2}$, where $\langle u^2 \rangle$ is the Debye-Waller factor, characterizing amplitude of the particle motion on the timescale of caging by neighboring particles. Specifically, we define $\langle u^2 \rangle$ as the value of the mean-squared displacement at time $t = 2$ for all $T$ and $\sigma$ (see Supplemental Material [31]). Figures 2(c) and 2(d) show the dependence of $\langle u^2 \rangle$ on $\sigma$ at $T = 0.45$ for both fixed and variable $\epsilon_{ma}$. The $\sigma$ dependence of $\langle u^2 \rangle$ does not mimic the $\alpha$-relaxation time. Curiously, the values of $\langle u^2 \rangle$ for monomers and additives intersect at $\sigma \approx 0.85$ for all cases, which corresponds to the $\sigma$ value of the crossing of polymer and additive $\tau$, thus suggesting a deeper connection.

To link the complex behaviors of $\tau$ and $\langle u^2 \rangle$, we turn to the localization model. In the LM, the $\alpha$-relaxation time $\tau$ is directly related to $\langle u^2 \rangle$ [20,21,32], indicating a connection between fast inertial dynamics occurring on a picosecond timescale and the long-timescale structural relaxation time. Specifically, the original formulation of the LM predicted $\tau = \tau_0 \exp\left(u_0^2/\langle u^2 \rangle\right)^{\alpha/2}$, where $\tau_0$, $u_0^2$, and $\alpha$ are model-dependent parameters; here we fix $\alpha = 3$, appropriate for an isotropic dynamic free volume. The LM has been validated in several systems with *no* free parameters by defining $\tau_0$ and $u_0^2$ from the values of $\tau$ and $\langle u^2 \rangle$ at a reference temperature [12,33,34]. Typically, this reference temperature is the onset temperature $T_A$ for non-Arrhenius temperature dependence on cooling [35]. However, this crossover temperature is not sharply defined and an unambiguous determination of $T_A$ is challenging. Moreover, there is no compelling reason why the onset of localization should arise at exactly the same temperature at which non-Arrhenius dynamics emerges. Accordingly, we consider an alternate characteristic temperature $T_\ell$ to define LM parameters, determined as a free empirical parameter for each $\sigma$. This approach for determining the characteristic temperature of the LM has also been used to examine the relaxation of the SPC/E model of water [36]. Defining $u_0^2$ and $\tau_0$ in terms of the reference values at $T_\ell$, the LM becomes

$$\tau(T) = \tau_\ell \, e^{-1} \, \exp\left[\left(\frac{u_\ell^2}{\langle u^2(T) \rangle}\right)^{3/2}\right], \tag{2}$$

where $\tau_\ell = \tau(T_\ell)$ and $u_\ell^2 = \langle u^2(T_\ell) \rangle$. The fact that $\langle u^2 \rangle$ and $\tau$ have different $\sigma$ dependencies at low $T$ implies that the characteristic parameters of the LM for all particle species must vary with $\sigma$. Figure 3 shows that LM prediction collapses to a linear master plot as a function of $(u_\ell^2/\langle u^2 \rangle)^{3/2}$ for polymer segments, additives, and all particles, for both fixed and variable monomer-additive interaction strength, demonstrating the success of the LM for each value of $\sigma$.

The variation of the LM parameters provides insight into what controls the changes in dynamics due to the additives. Figures 4(a) and 4(b) show the variation of $u_\ell^2$ and $\tau_\ell$ with $\sigma$. The most striking observation is that the $\sigma$ dependence of the model parameters is nearly identical for the cases of fixed and variable $\epsilon_{ma}$, which requires that the $T$ dependence of $\tau$ at a given $\sigma$ is identical (relative to an $\epsilon_{ma}$-dependent reference temperature). In other words, the functional form of the $T$ dependence is determined *solely* by the additive size. Since we know from Fig. 2 that the $\sigma$ dependence of $\tau$ is different for fixed versus variable $\epsilon_{ma}$, the information about the monomer-additive interactions must be encoded solely in the variation of the reference temperature $T_\ell$. Indeed,

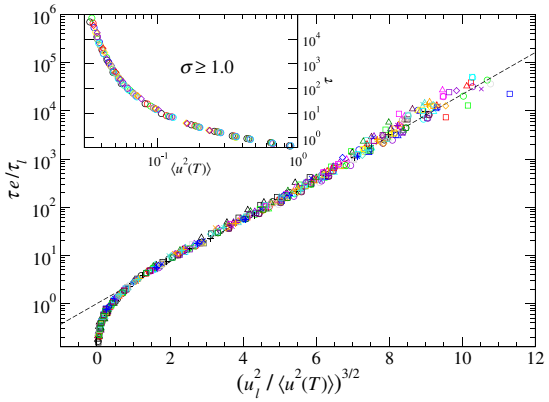


FIG. 3. Data collapse for the relaxation time $\tau$ using the localization model [Eq. (2)] for polymer segments (circles and diamonds), additives (triangles and stars), combined system (squares and x-es), and pure system (crosses) for both fixed and varying $\epsilon_{ma}$. Data for each $\sigma$ are different colors, and the dashed line indicates the predicted data collapse. The inset shows the monomer alpha relaxation time $\tau_m$ as a function of $\langle u^2 \rangle$ for various $\sigma \geq 1.0$ and $T$ using both fixed and variable $\epsilon_{ma}$. The collapse of these data without scaling indicates the LM parameters are independent of $\sigma$ for $\sigma \geq 1.0$.

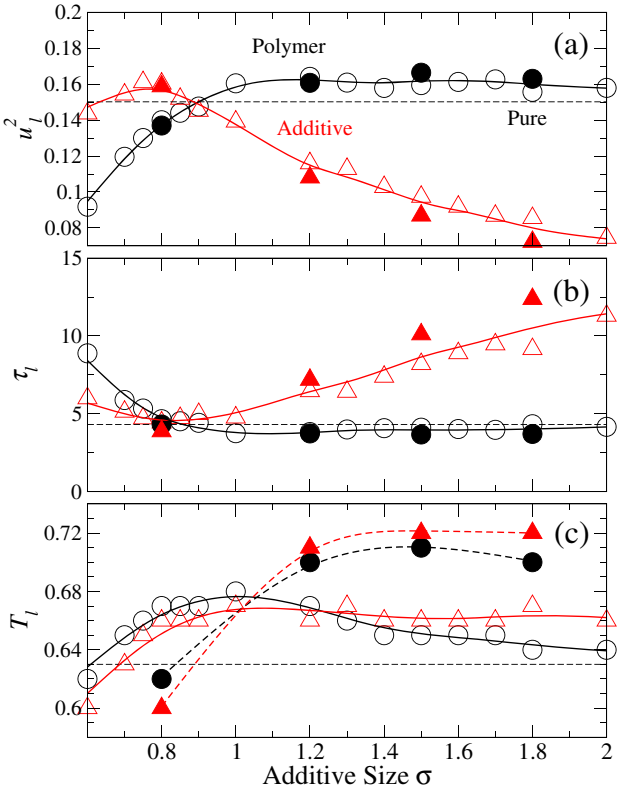


FIG. 4. The localization model parameters (a) $u_\ell^2$, (b) $\tau_\ell$, and (c) $T_\ell$ as a function of $\sigma$ for polymer (circles), additive (triangles), and the pure polymer reference case (horizontal line). The open symbols are for fixed $\epsilon_{ma}$, and filled symbols are for increasing $\epsilon_{ma}$ with size; $u_\ell^2$ and $\tau_\ell$, which determine the $T$ dependence of $\tau$, are nearly independent of $\epsilon_{ma}$. Note that $\tau_\ell$ and $u_\ell^2$ for polymers are approximately constant for $\sigma \geq 1$. Other than the reference pure polymer, lines are only a guide for the eye.

Fig. 4(c) shows the variation of $T_\ell$ is quite different for the cases of fixed and variable $\epsilon_{ma}$. Thus, additive size controls the functional form of the $T$ dependence, while additive interactions control the onset temperature of localization.

The variation of $u_\ell^2$ and $\tau_\ell$ with additive size provides further insight into the variation of dynamics with $\sigma$. As noted for the $\sigma$ dependence of $\tau$ and $\langle u^2 \rangle$ (Fig. 2), the $\tau_\ell$ and $u_\ell^2$ values for polymer and additives cross at $\sigma \approx 0.85$. Furthermore, $\tau_\ell$ and $u_\ell^2$ at $\sigma \approx 0.85$ match the corresponding values of the pure polymer system, emphasizing a characteristic size scale close to that of the polymer segments. At $\sigma \approx 0.85$, the additive systems have identical $T$ dependence to the pure polymer system, but with an overall shift in the temperature scale because of the differences in $T_\ell$. Figures 4(a) and 4(b) also show that $\tau_\ell$ and $u_\ell^2$ for the polymer reach approximately constant values for $\sigma \geq 1.0$. A constant value for the LM parameters requires that $\tau$ is a universal function of $\langle u^2 \rangle$ for $\sigma > 1.0$ without any renormalization. The inset of Fig. 3 confirms data collapse without renormalization in this $\sigma$ range. This is in-line with arguments in earlier literature [8,10,37] that the changes in dynamics due to NPs can be directly related to dynamical changes in thin films. In other words, the approach of $\tau_\ell$ and $u_\ell^2$ to an asymptotic value suggests that we reach this macroscopic interface limit when the additive size roughly exceeds that of the polymer segments. We also analyzed data from earlier polymer-NP composite simulations with variable NP size from Ref. [30] and confirmed that the LM parameters also asymptote to fixed values for larger NP size (see Supplemental Material [31]), supporting this assertion. Previous work on polymer thin films [38,39] found that the mobility changes of films are dominated by changes of the high-$T$ activation free energy. In the Supplemental Material [31], we show that, similar to films, there is a significant alteration of the high-$T$ activation barrier with additive size, which partially accounts for the $\sigma$-dependent changes in the $T$ dependence of $\tau$.

We have shown that the addition of additives to a polymer melt with sizes ranging from small molecules to nanoparticles can result in complex changes to the $\alpha$-timescale dynamics. For additive sizes smaller than the polymer segments, the effects of additives diminish rapidly. From a quantitative view, we have shown that the localization model describes the complex size dependence of $\tau$, even though the size dependence of $\langle u^2 \rangle$ is comparatively simple and monotonic. The LM parameters $\tau_\ell$ and $u_\ell^2$ appear to depend only on additive size and are insensitive to the strength of polymer interactions with the additives, indicating an entropic origin to the changes in $T$ dependence; interaction strength only affects the temperature $T_\ell$ at which localization becomes significant. For additive sizes larger than the polymer segment size, the LM parameters saturate,

demonstrating that a fixed relationship emerges at a surprisingly small additive size and extends to much larger NP additives. This accounts for the observation that the changes in polymer dynamics due to NP can be mapped for different NP sizes, ranging up to the limit of thin films. A natural extension of these findings includes considering more complex additive shapes, which may affect some of the findings presented here; some work has already been done in this direction [12,40]. More generally, these findings are useful for applications in which diluents are commonly used to alter the plasticity of materials.

We acknowledge funding support from NIST Award No. 70NANB15H2.

[1] K. I. Winey and R. A. Vaia, MRS Bull. **32**, 314 (2007).
[2] M. Muhammed Shameem, S. Sasikanth, R. Annamalai, and R. Ganapathi Raman, Mater. Today **45**, 2536 (2021).
[3] L. Mascia, Y. Kouparitsas, D. Nocita, and X. Bao, Polymers **12**, 769 (2020).
[4] M. T. Cicerone and J. F. Douglas, Soft Matter **8**, 2983 (2012).
[5] G. Caliskan, D. Mechtani, J. H. Roh, A. Kisliuk, A. P. Sokolov, S. Azzam, M. T. Cicerone, S. Lin-Gibson, and I. Peral, J. Chem. Phys. **121**, 1978 (2004).
[6] R. El Moznine, G. Smith, E. Polygalov, P. M. Suherman, and J. Broadhead, J. Phys. D **36**, 330 (2003).
[7] G. A. Salvatore, N. Munzenrieder, T. Kinkeldei, L. Petti, C. Zysset, I. Strebel, L. Buthe, and G. Troster, Nat. Commun. **5**, 2982 (2014).
[8] F. W. Starr, T. B. Schroder, and S. C. Glotzer, Phys. Rev. E **64**, 021802 (2001).
[9] F. W. Starr, J. F. Douglas, D. Meng, and S. K. Kumar, ACS Nano **10**, 10960 (2016).
[10] A. Bansal, H. Yang, C. Li, K. Cho, B. C. Benicewicz, S. K. Kumar, and L. S. Schadler, Nat. Mater. **4**, 693 (2005).
[11] S. Cheng, X. Shi-Jie, J.-M. Y. Carrillo, B. Carroll, H. Martin, P.-F. Cao, M. D. Dadmun, B. G. Sumpter, V. N. Novikov, K. S. Schweizer, and A. P. Sokolov, ACS Nano **11**, 752 (2017).
[12] J. H. Mangalara and D. S. Simmons, ACS Macro Lett. **4**, 1134 (2015).
[13] E. M. Zirdehi and F. Varnik, J. Chem. Phys. **150**, 024903 (2019).
[14] R. A. Riggleman, J. F. Douglas, and J. J. de Pablo, Soft Mat. **6**, 292 (2010).
[15] R. A. Riggleman, J. F. Douglas, and J. J. de Pablo, J. Chem. Phys. **126**, 234903 (2007).
[16] E. M. Zirdehi, T. Voigtmann, and F. Varnik, J. Phys. Condens. Matter **32**, 275104 (2020).
[17] T. C. Merkel, B. D. Freeman, R. J. Spontak, Z. He, I. Pinnau, P. Meakin, and A. J. Hill, Science **296**, 519 (2002).
[18] T. C. Merkel, B. D. Freeman, R. J. Spontak, Z. He, I. Pinnau, P. Meakin, and A. J. Hill, Chem. Mater. **15**, 109 (2003).
[19] A. L. Andrady, T. C. Merkel, and L. G. Toy, Macromolecules **37**, 4329 (2004).
[20] A. Ottochian and D. Leporini, J. Non-Cryst. Solids **357**, 298 (2011).
[21] D. S. Simmons, M. T. Cicerone, Q. Zhong, M. Tyagi, and J. F. Douglas, Soft Matter **8**, 11455 (2012).
[22] K. L. Ngai, L.-R. Bao, A. F. Yee, and C. L. Soles, Phys. Rev. Lett. **87**, 215901 (2001).
[23] S. Plimpton, J. Comput. Phys. **117**, 1 (1995).
[24] Y. Katoka and Y. Yamada, J. Comput. Chem. Jpn. **14**, 10 (2015).
[25] F. Cuadros, I. Cachadiña, and W. Ahumada, Molecular engineering **6**, 319 (1996).
[26] H. Wang and M. Frenklach, Combust. Flame **96**, 163 (1994).
[27] J. Hirschfelder, C. F. Curtiss, and R. B. Bird, *Molecular Theory of Gases and Liquids* (John Wiley and Sons, New York, 1964).
[28] S. Peter, H. Meyer, and J. Baschnagel, J. Polym. Sci. Part B **44**, 2951 (2006).
[29] P. Z. Hanakata, B. A. Pazmiño Betancourt, J. F. Douglas, and F. W. Starr, J. Chem. Phys. **142**, 234907 (2015).
[30] H. Emamy, S. K. Kumar, and F. W. Starr, Phys. Rev. Lett. **121**, 207801 (2018).
[31] See Supplemental Material at http://link.aps.org/supplemental/10.1103/PhysRevLett.127.277802 for further details on the structure and dynamics of the material.
[32] C. Forrey, D. M. Saylor, J. S. Silverstein, J. F. Douglas, E. M. Davis, and Y. A. Elabd, Soft Matter **10**, 7480 (2014).
[33] B. A. Pazmino Betancourt, P. Z. Hanakata, F. W. Starr, and J. F. Douglas, Proc. Natl. Acad. Sci. U.S.A. **112**, 2966 (2015).
[34] W. Xia, J. Song, N. K. Hansoge, F. R. Phelan, S. Keten, and J. F. Douglas, J. Phys. Chem. B **122**, 2040 (2018).
[35] S. Sastry, P. Debenedetti, and F. Stillinger, Nature (London) **393**, 554 (1998).
[36] R. Horstmann and M. Vogel, J. Chem. Phys. **147**, 034505 (2017).
[37] L. Schadler, S. Kumar, B. Benicewicz, S. Lewis, and S. Harton, MRS Bull. **32**, 335 (2007).
[38] W. Zhang, F. W. Starr, and J. F. Douglas, J. Phys. Chem. B **123**, 5935 (2019).
[39] W. Zhang, F. W. Starr, and J. F. Douglas, J. Chem. Phys. **152**, 124703 (2020).
[40] M. Becchi, A. Giuntoli, and D. Leporini, Soft Matter **14**, 8814 (2018).